# Trade-offs between hydrogen production and hydropower flexibility in a Swedish power system with high shares of renewables

Christian Mikovits[a,*], Elisabeth Wetterlund[b,c], Johann Baumgartner[a], Sebastian Wehrle[a], Johannes Schmidt[a]

[a] *Institute for Sustainable Economic Development, University of Natural Resources and Life Science, Vienna, Austria*
[b] *Energy Engineering, Division of Energy Science, Luleå University of Technology, 971 87 Luleå, Sweden*
[c] *International Institute for Applied Systems Analysis (IIASA), A-2361 Laxenburg, Austria*

**Abstract**

Hydrogen produced from renewable electricity can play an important role in deep decarbonisation of industry such as steel-production. Hydrogen production can also be a source of negative balancing capacity to increase flexibility of fully renewable power systems. However, there is a trade-off between attaining economically favorable high full-load hours for the electrolyzer and providing flexibility to the system. To better understand this trade-off in a system with high amounts of hydropower generation, we apply a dispatch model for the Swedish power system to 29 different weather years, in order to simulate weather-dependent electricity generation (hydro and wind) and demand at hourly temporal resolution. Thus, we are able to represent extreme weather events. We fix hydropower and thermal power capacities and only increase wind power installations. Under the assumption of low hydropower flexibility capacities due to environmental restrictions and no dispatch of thermal power for hydrogen production, electrolyzers operate at above 60 % of full-load hours. With higher hydropower flexibility, full load hours increase by up to 10 percentage points; in particular with thermal dispatch for hydrogen production, where over 90 % full-load hours are possible. The interannual variability of hydrogen production is high in all considered scenarios, which shows that the demand side flexibility for hydrogen users will also be important.

*Keywords:* renewables, `hydrogen`, flexibility, biomass, long-term analysis

## 1. Introduction

Hydrogen is considered as one important option for deep decarbonization of energy and industrial sectors, in particular in the fields of transportation [1], as feedstock for fuel or chemical production, as reductant in primary steel-making [2], or as energy storage in stationary heat and electricity applications [3–5]. Today, natural gas, through steam methane reforming, constitutes the primary source for hydrogen production [6]. With decreasing costs of renewable electricity generation and

*Corresponding author
*Email addresses:* `christian.mikovits@boku.ac.at` (Christian Mikovits), `elisabeth.wetterlund@ltu.se` (Elisabeth Wetterlund), `johann.baumgartner@boku.ac.at` (Johann Baumgartner), `sebastian.wehrle@boku.ac.at` (Sebastian Wehrle), `johannes.schmidt@boku.ac.at` (Johannes Schmidt)

the need to switch to carbon-free energy carriers [7], the interest for hydrogen produced via water electrolysis using low-carbon electricity is, however, rapidly increasing [8, 9].
Sweden is well positioned to take a lead position in the production of low-carbon hydrogen, as it has a power system with one of the globally lowest $CO_2$-emission footprints, and strong policies in place to support full decarbonization: Sweden targets reaching zero net emissions of greenhouse gases to the atmosphere by 2045, with a goal of 100 % renewable electricity production by 2040 [10]. Hydrogen is being outlined as a potential key technology in the future Swedish energy system, where it can play several roles: as a flexibility technology to balance a high share of variable renewable energy (VRE) in the power system, for production of hydrocarbons and in the biofuel sector, and as reductant in the steel industry, where hydrogen is currently considered as the main track for decarbonization of primary steel-making [11–13]. In order to be able to significantly expand hydrogen production from electricity in Sweden, while concurrently phasing out nuclear power, which currently provides approximately 40% of the total generation [14], additional sources of low-carbon electricity generation are necessary. As hydropower (supplying another 40% of the total Swedish generation) is almost at its full potential, solar PV is unlikely to be developed significantly in Sweden due to low solar radiation, and power from CHP (combined heat and power) plants using renewable fuels is inherently restricted by the available heat loads, wind power becomes the main source for an expansion of renewable electricity generation [12, 15]. Additionally, the potential is likely to increase in Scandinavia due to positive trends in wind speeds according to recent climate projections [16, 17].

Wind power, however, is non-dispatchable and therefore adds variability to the system. Hydropower is arguably the single most important source of flexibility in the Nordic power system, as it offers flexibility on all time-scales, from hours to seasons [18]. With increased shares of VRE in the power system, hydropower is expected to gain further importance, as sudden changes in the power balance will most likely be compensated for by varying the hydropower operation. The existing hydropower system is in principle able to balance the additional variability of a high share of VRE production for the current load [19], but increased loads from decarbonization measures, such as electrification of industry and transportation, may shift the balance due to the need of further increased wind power capacities. For carbon free hydrogen production, full-load hours of electrolyzers should be kept at a high level due to the economics of hydrogen production [20], which, in combination with high VRE shares, may put additional strains on the hydropower regulating system. A particular risk for conflicts with other environmental quality objectives lies in increased rapid sub-daily fluctuations in water flow and water levels (*hydropeaking*), as short-term river regime alteration poses a key threat to river ecosystems [21–24]. Hydropeaking has been observed as both high and increasing in Nordic regulated rivers [22, 25], and in order to prevent adverse impacts on river ecosystems, environmental impacts of using hydropower for load balancing must be better understood in order to help policy-makers set environmentally sustainable limits [22, 26, 27]. For Swedish conditions, a national strategy has been proposed for managing the trade-offs between measures that reduce the environmental impact of the hydropower, and measures that enable increased production to meet future needs in the energy system [28, 29]. The strategy does not, however, specifically target the issues related to anthropogenic-induced rapid flow fluctuations. It is thus necessary to further investigate the interactions in the power system if more stringent regulations were to be put in place to prevent adverse impacts on river ecosystems due to hydropeaking and water retention throughout low flow seasons [26].

Other studies have already shown the potential to use excess wind power to produce hydrogen as a transport fuel in relation to a limited electricity network [30]. Focus has, however, typically been on the combination of wind power and hydrogen as a measure for electricity storage and wind curtailment mitigation [31–33]. Assessing hydro-thermal-wind systems and their interactions with hydrogen production has, to the best of our knowledge, not been previously published.

We therefore assess here the interactions in a power system with high shares of VRE between large-scale expansion of wind power, possibilities to produce renewable hydrogen via electrolysis, and the existing power production in the system. Our overall aim is to identify and analyse the trade-offs between the amount of thermal power generation, full-load hours of electrolyzers, impacts on river flows of hydropower operation, and the need for additional backup flexibility options.

The study is performed as a case study for Sweden, but the results will be relevant also for other regions with high shares of hydropower and high and increasing shares of VRE.

The variability of weather in both short and long term periods is fundamental to understand these trade-offs, as temperature drives load, and wind speeds and precipitation determine wind and hydropower generation, respectively. In order to be able to realistically capture extreme weather events, we use simulations of time series of VRE and electricity demand in a dispatch model for the Swedish power system for 29 different weather years, at hourly temporal resolution. We can thus assess how both short-term (hours to days) and long-term (days to months to years) variability of climatic variables drive the power production patterns. The model was developed by Höltinger et al. [19], who used it to assess the impacts of climatic extreme events on the feasibility of fully renewable power systems, using Sweden as a case study. The model is here extended by hydrogen technology and a more detailed representation of thermal power generation and hydropower operational restrictions.

## 2. Material and methods

We assess different scenarios for hydrogen demand, hydrogen value and hydropower flexibility, using a power system model for Sweden. In the following section, we present the general model structure and most relevant parts, as well as the major changes compared to the work by Höltinger et al. [19], with a more comprehensive and detailed model description given in Appendix A.1.

### *2.1. Dispatch model and data*

#### *2.1.1. Model description*

The optimization model runs with hourly data for natural river runoff, load and wind generation and aims to minimize the variable system costs. The objective function consists of the sum of the costs of generation, taking into account also the value of produced hydrogen. The residual demand, i.e. the difference between wind power generation and load, has to be balanced by thermal and hydropower generation, curtailment and spilling of water. Thus, the need for potential additional backup measures is also captured. The backup measures were assumed to be available at very low investment but high variable costs, as they are used with low frequency. Candidates are additional thermal peaking plants, demand side management measures, or imports from neighboring countries, which might also be stressed by a climatic extreme event.

To be able to account for climate variability, the model was run for 29 different weather years, which were used to simulate *load*, *hydropower*, and *wind power* generation in the model. The model optimizes a single year of dispatch with no transfer of parameters from one year to another, i.e., interannual water storage was not considered. The electricity demand was modelled using a regression model, reanalysis temperature data for 29 years, and gridded population raster data, in

Table 1: Costs and capacities used. (CHP = combined heat and power, RDF = refuse derived fuel, NG = natural gas, NGCC = natural gas combined cycle, FST = condensing steam turbine, OCGT = open cycle gas turbine, IC = internal combustion engine, S = small, M = medium, L = large, I = industrial.)

| | Production type | Fuel type | Installed capacity (MW) | Costs (€ $MWh^{-1}$) |
|---|---|---|---|---|
| Thermal Plants | Waste (CHP) | Waste | 315 | -63.2 |
| | RDF (CHP) | Waste | 385 | 5.55 |
| | Biomass I (CHP) | Biomass | 1,255 | 18.8 |
| | Biomass L (CHP) [a] | Biomass | 1,318 | 21.0 |
| | Biomass M (CHP) | Biomass | 603 | 24.8 |
| | Biomass S (CHP) | Biomass | 401 | 30.9 |
| | NGCC L (CHP) | NG | 701 | 57.9 |
| | NGCC M (CHP) | NG | 54 | 74.1 |
| | NG IC (CHP) | NG | 13 | 83.4 |
| | FST | Oil & NG | 905 | 125 |
| | OCGT | Oil | 1,579 | 152 |
| | Biogas IC (CHP) | Biogas | 21 | 156 |
| | Hydro | - | 16,200 | 1 |
| | Wind | - | varying [b] | 0 |
| | Additional backup measures | - | - | 1,500 |
| | Electrolysis | - | varying [b] | varying |

[a] This category also contains CHP plants currently using coal or peat as fuel (total installed capacity of 298 MW), as those were assumed to have been replaced by biomass CHP.

[b] Wind and electrolysis capacity are directly coupled, detailed explanation in section 2.2.1

order to obtain a temperature dependent load profile based on population weighted mean temperatures (for details see Höltinger et al. [19]). The modelled annual load follows the current power demand (approximately 130 TWh $a^{-1}$, excluding transmission losses). We have only considered increased power demand from electrolysis (see section 2.2.1), and not from other sectors or users (e.g., increased electrification of the transport sector, electrification of other parts of the industry, or data-centers).

Table 1 summarizes the characteristics for the included power plant types and other model components.

### *2.1.2. Wind power*

For wind power, we used time series for potential future wind power production in Sweden, as modelled by Olauson et al. [34, 35]. The authors generated a range of different scenarios, based on bias corrected data for Sweden. We have here assumed that the nuclear power production, i.e. 60-65 TWh $a^{-1}$ from 8.6 GW of installed capacity [14], is fully phased out and replaced by wind power. We also assumed a reduction of power exports to zero, which can be compared to historical net exports which varied between 7.2 and 23 TWh $a^{-1}$ during the years 2011-2018 [14]. Further we accounted for a certain minimum thermal production from CHP plants (see section 2.1.4). This gives a total average annual wind power production of 49 TWh $a^{-1}$ from 14 GW of installed capacity, in the base scenario without hydrogen production, which can be compared to the current annual production of 17 TWh $a^{-1}$ from 7.4 GW of installed capacity (in 2018) [14]. The higher full load hours for new generation can be attributed partly to offshore wind capacities, and partly to larger rotor sizes, which decreases the specific power of turbines.

In the modelled electrolysis scenarios, wind generation was scaled to match the increased demand, as described in section 2.2.1.

*2.1.3. Hydropower*

We followed the previous model formulation given in Höltinger et al. [19], which assumed a simplified hydropower model aggregating all hydropower plants to one reservoir and one plant. Simulated time series for river discharge from the hydrological catchment model S-HYPE were used [36, 37] and translated into power generation with a simulation model that takes the characteristics of all Swedish hydropower plants into account. A total reservoir capacity of 33.7 TW h was modelled, which needs to be kept between minimum (5 %) and maximum (98 %) observed levels during all hours [19, 38].

The reservoir level at the start of each year, as well as the required minimum level at the end of the year, were both set to 62 %, which corresponds to the average reservoir filling level for the time period of 1960 to 2016 [38]. This represents a rather conservative approach which limits the possibility for hydropower to act as interannual storage, as extreme weather years with, e.g., low production of both hydro and wind power, cannot be dealt with by running down the levels of hydropower reservoirs at the end of the year. Historically, end-of-year reservoir levels have seen variation between 43 % and 86 % [38].

Hydropower operational limits, i.e., minimum flows and maximum ramping rates, were then assessed in two different scenarios (see section 2.2.3).

*2.1.4. Thermal power generation*

Höltinger et al. [19] did not differentiate between plant and fuel types; instead, thermal power generation was defined as one plant. We have here improved the original thermal generation model by disaggregating it into different plant technologies and fuel types.

Data on existing thermal power generation was compiled from the World Electric Power Plants database [39], and complemented by national statistics [40, 41]. The thermal production was categorised based on fuel, production scale and production technology, with each plant type defined by individual marginal generation costs and capacities (Table 1). Power production costs were set based on bottom-up technology and fuel specific projections of electricity generation costs. The production costs include fuel costs including a $CO_2$-charge (50 € /$\text{ton}_{CO_2}$), costs for operation and maintenance, and heat credits, when applicable. Appendix A.2 provides the details on the applied costs and plant efficiencies.

We have additionally defined must-run conditions for different seasons of the year, as many plants are associated with heat demand for housing and industry. Generation in CHP plants was assumed to follow a monthly pattern throughout each year, with higher minimum production during the winter months, and lower minimum production during the summer. Additionally, maximum production was restricted during the summer period to account for maintenance and limited operation of CHP plants due to heat load restrictions. The annual production profiles were developed based on statistics of installed capacity and annual production per fuel type, in district heating systems and industrial back-pressure systems, respectively [38]. Expected annual full-load hour equivalents amount to 7500 h $a^{-1}$ for industrial biomass CHP and waste CHP, and 5000 h $a^{-1}$ for biomass CHP plants [42]. The load profiles applied in the optimization model are shown in Figure 1.

Maximum combined hourly ramping rates for the sum of thermal power generation were derived from historical observations of maximum ramping rates, and therefore set to 1.5 GW.

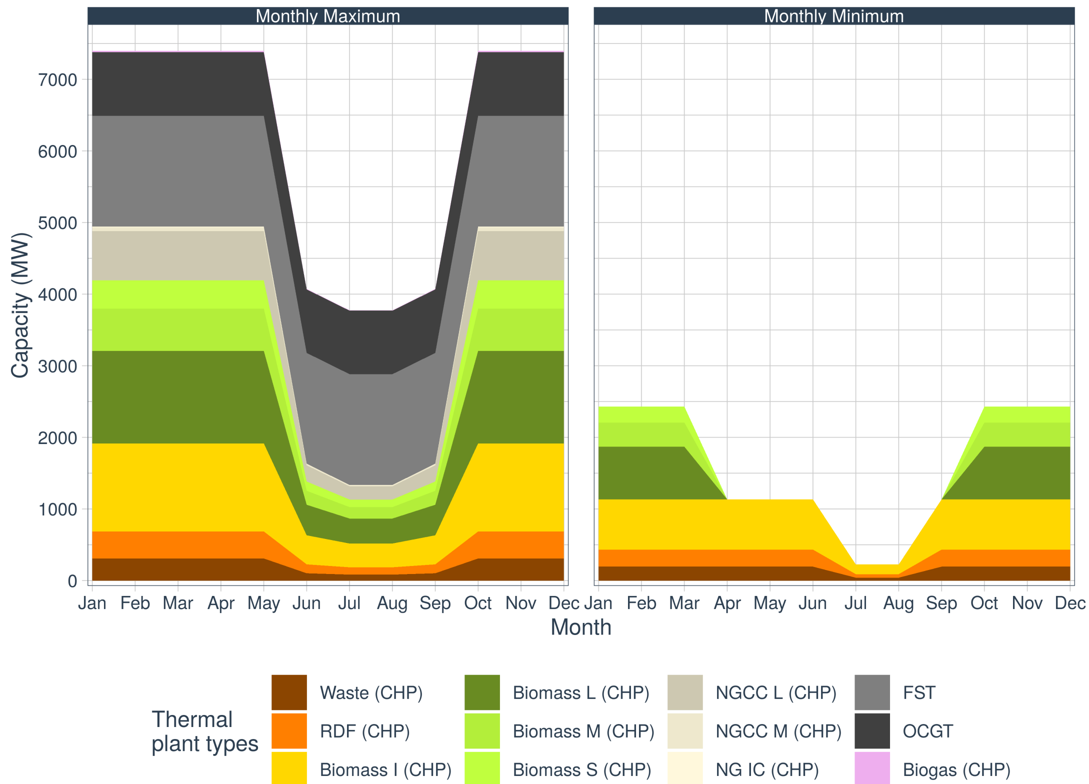


Figure 1: Modelled maximum (left) and minimum (right) thermal power production, per category.

*2.1.5. Hydrogen production*

We have assumed that electrolyzer technology will advance beyond the current state-of-the-art (alkaline electrolysis), to proton exchange membranes (PEM). This has been reflected in our assumptions on hydrogen production efficiency, which was set to 72 % (system efficiency, defined as hydrogen output on LHV basis divided by electrical input to the electrolysis system), corresponding to 46 kWh of electricity per kg hydrogen [43–45]. The electrolyzer was sized according to an expected electrolyzer availability of 90 %. As described in section 2.2.1, the full-load hours of the electrolyzer are actually a model output, which means that the hydrogen demand in the different scenarios will not always be exactly met.

As PEM electrolyzers in general are very flexible, with start-up times in the range of minutes or even seconds and very low minimum part-load operation (<10 %), neither ramping nor electrolyzer part-load restrictions were considered in the model [45].

*2.2. Scenarios*

In order to assess the potential trade-offs between flexible hydropower operation, thermal power generation, and electrolyzer operation, we have created scenarios with variations of three key parameters; *(i)* total hydrogen demand from electrolysis (4 scenarios), *(ii)* value of hydrogen (2 scenarios), and *(iii)* allowed hydropower flexibility (2 scenarios). This results in a total of 14 scenarios as the baseline scenarios do not include hydrogen production and therefore no hydrogen value scenarios. Additionally, we ran the model in a sensitivity analysis for a wider set of hydrogen demands (see section 2.2.1).

*2.2.1. Hydrogen demand*

The hydrogen production scenarios were chosen so that they are able to deliver different amounts of hydrogen in order to satisfy different levels of future projected demands. We limited the hydrogen usage options to two pathways that are currently under development in Sweden: for hydrotreatment of different bio-based feedstocks in biofuel production, and as use as reductant in fossil-free primary steel-making according to the HYBRIT (Hydrogen Breakthrough Ironmaking Technology) route. We applied four different hydrogen scenarios, where one is the baseline scenario without electrolysis-based hydrogen, and the other three can be seen to represent either different ambition levels for decarbonization, or different time perspectives. This results in different electrolysis loads on the system, as outlined in Table 2.

Table 2: Modelled hydrogen demand scenarios.

| Scenario | Hydrogen for biofuels (TWh $a^{-1}$) | Hydrogen for steel-making (TWh $a^{-1}$) | Electrolyzer capacity (MW) |
|---|---|---|---|
| NO | 0 | 0 | 0 |
| LOW | 5 | 0 | 880 |
| MID | 10 | 0 | 1760 |
| HIGH | 10 | 10 | 3610 |

The estimates regarding biofuel production build on the ambitions announced by Preem, Sweden's largest fuel producer, who have a goal of producing 3 million m$^3$ of biofuels by 2030 in their two refineries in Sweden [46]. Judging from their announced projects and plans, all biofuels will be drop-in fuels produced via hydroprocessing of various bio-crudes. Hydrogen is currently produced from refinery off-gases or via steam reforming of natural gas, but Preem has also expressed strong interest in hydrogen produced via electrolysis [46]. We have based our scenarios on the assumption that electrolysis-based hydrogen will be the main pathway in the future, and implement two different annual demand levels; 5 and 10 TWh $a^{-1}$ hydrogen, respectively. The lower level represents a scenario where a large share of the biofuel feedstock has a relatively low oxygen content (e.g., used cooking oils or bio-crudes produced via hydroypyrolysis or hydrothermal liquefaction), while the higher scenario assumes a large share of biofuel feedstock with a higher oxygen content (e.g., lignin oil or fast pyrolysis oil) [47, 48].

In the HIGH scenario, we also assumed that the HYBRIT route will be fully implemented in Sweden, and that all primary steel-making via the blast furnace-basic oxygen furnace route will thus be replaced with hydrogen based direct reduction followed by electric arc furnaces. We only considered the projected additional electricity demand to cover the required hydrogen production

($10\,\mathrm{TWh}\,a^{-1}$) [13, 49], while the additional electricity demand from downstream processes was excluded, similar as to other industrial electrification (see section 2.1.1).

The scenarios were implemented by changing the restriction on electrolyzer capacity and scaling the wind power accordingly. We chose the scaling in a way so that on average, wind power generates enough electricity to supply the electrolyzer at full load, i.e., in an 880 MW electrolyzer scenario, we added wind capacity which on average generates $880\times8760\,\mathrm{MWh}\,a^{-1}$. Thus, we can assess in how far the wind resource can be used for electrolysis and how much of the wind is curtailed. Electrolyzer full-load hours are thus an output of the model, which means that the total defined hydrogen demand may not be exactly met in all scenarios, if it is too costly to do so.

In addition to the scenarios based on actual announced plans by different industrial actors, we applied a sensitivity analysis, where we tested extended capacities of electrolyzers - and associated increases in wind power generation - on a wide range of scenarios (5000 MW to 100,000 MW).

### *2.2.2. Hydrogen value*

Additionally to varying the hydrogen demand, we also assessed the impact of dispatching thermal for hydrogen production. Technically, we did so by varying the value of hydrogen so that it was either below most ($18\,€\,\mathrm{MWh}^{-1}$) or above all ($160\,€\,\mathrm{MWh}^{-1}$) marginal costs of thermal generation. Thus, thermal power was either never or always dispatched to produce hydrogen. This represents two extreme settings, for which reason the results cover a wide range of possible outcomes.

### *2.2.3. Hydropower flexibility*

We assessed two different scenarios regarding the impact of seasonal ramping restrictions and seasonal flow thresholds in the hydropower system, that represent two different hydropower regulation development pathways. The first scenario allows for high flexibility in the hydropower operation, including the possibility for rapid flow fluctuations *(High hydropower flexibility, HHF)*. The second scenario represents a more cautious scenario designed to prevent adverse impacts on river ecosystems from hydropeaking and water retention throughout low flow seasons *(Low hydropower flexibility, LHF)*. The restrictions were implemented by limiting the maximum ramping rate (MRR) and minimum flow (MF), following the approach proposed by Olivares et al.[50]. MF1 is a rather unrestricted scenario at 20 % of median natural flow, while MF2 is very restrictive at 50 %. The maximum ramping rate MRR1 is at 28 % of median natural flow, with MRR2 at only 6 %. MF1 and MRR1 were combined in the HHF scenario, and MF2 and MRR2 in the LHF scenario.

The resulting monthly values are displayed in figure 2, where *a* shows the minimum flow, and *b* the maximum ramping rates. All values were derived from the simulation of potential natural flows (i.e., without human intervention) from the S-HYPE model [36, 37]. We observe the highest monthly median flow in June at about 18,000 MW, and the lowest flow in March, at only 3600 MW, which leads to a high variation throughout the year of both minimum flows and maximum ramping rates. Figure 2 *a* also shows the historical daily mean flows of all the 29 modelled weather years (blue) and the daily mean of 16 modelled weather years with regulated (human interference) flow (yellow).

### *2.3. Model runs and performance indicators*

We ran the optimization model for all scenarios outlined in the previous sections. Each scenario was evaluated for the 29 different weather years, at an hourly temporal scale. Our evaluation focused on the following performance indicators:

- Average full-load operations of electrolyzers (% of 8,760 hours)

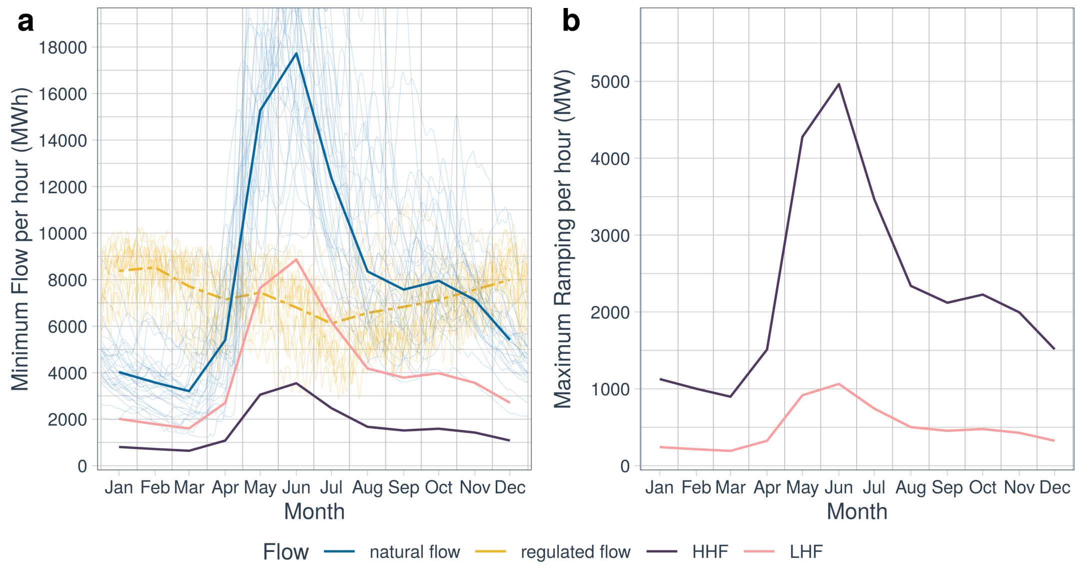


Figure 2: $a$: Minimum flow per hour (expressed as MWh $h^{-1}$), and $b$: Maximum allowed ramping per hour (expressed as MW $\mathrm{h}^{-1}$), for the two modelled flexibility scenarios. $a$ also shows the daily mean flows of all 29 weather years: natural and regulated. HHF = High hydropower flexibility, LHF = Low hydropower flexibility.

- Interannual variability of hydrogen production (variance in full-load operation)
- Required additional backup capacity (MW)
- Required additional backup volume (MWh $a^{-1}$)
- Dispatched thermal power generation (MWh $a^{-1}$)
- Variability in hydropower flow (max ramping per hour) (MW)
- Minimum hydropower flow (MW)

## 3. Results

The results focus on the interactions of electrolyzer operation for production of renewable hydrogen with large-scale expansion of wind power (section 3.1), as well as on the need for thermal power production and additional backup (section 3.2), and hydropower production and flexibility (section 3.3). Section 3.4 presents a summarizing analysis of the different trade-offs involved in the system, and section 3.5 an extended sensitivity analysis of electrolyzer full-load hours regarding total electrolyzer capacity.

### *3.1. Hydrogen production and wind power expansion*

Figure 3 shows the average electrolyzer full-load operation for all 29 modelled weather years as a function of installed electrolyzer capacity, while figure 4 shows the same results but as a box plot of all 29 different weather years, in order to be able to catch the interannual variability of the

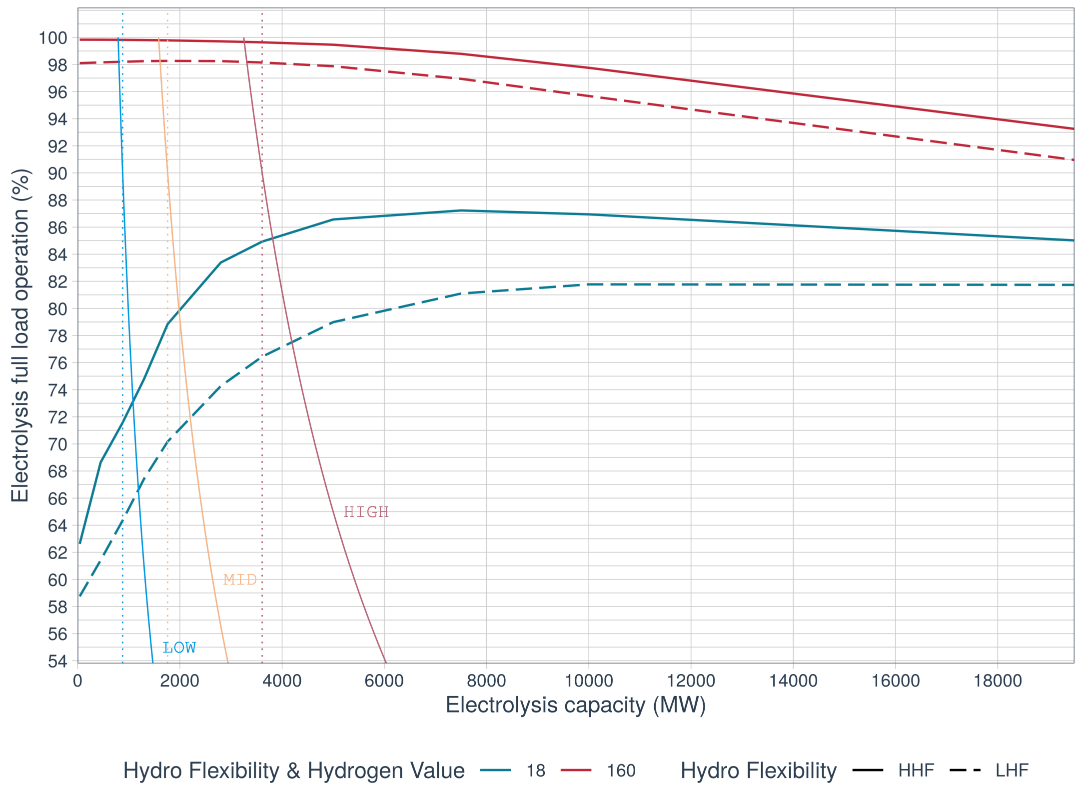


Figure 3: Average electrolyzer full-load operation (%) for an extended electrolyzer capacity range, for both hydropower flexibility scenarios: LHF and HHF, and for both hydrogen value scenarios: no thermal (18 € $\mathrm{MWh}^{-1}$) and thermal dispatch (160 € $\mathrm{MWh}^{-1}$). The three hydrogen demand scenarios are marked with vertical dotted lines, the curved lines shows the adjusted electrolyzer capacity to meet the expected yearly production (estimated at 90 % for each scenario).

electrolyzer operation. Both figures shows results for an extended electrolyzer capacity range. As has been described, the wind power generation increases accordingly in the scenarios.

The first thing that can be learnt from the figures is that, as expected, the full-load hours decrease if (a) the hydropower flexibility decreases, and (b) the assumed hydrogen value is reduced. The scenarios with low hydrogen value (no thermal dispatch) exhibit a substantial difference between the two hydropower flexibility scenarios (LHF and HHF), where the full-load hours drop by up to 10 percentage points. This impact is much less significant for the scenario with high hydrogen value, because thermal power is here dispatched to not only balance residual demand, but also to power the electrolysis.

Secondly, the lower hydrogen value results in a strong dependency on the weather year (high spread), which decreases (lower spread) with increasing hydrogen demand (see figure 4). Conversely, the high-value hydrogen scenarios exhibit very little weather dependency overall, but with a spread that increases with increasing hydrogen demand. Unsurprisingly, the weather dependency is more pronounced with less hydropower flexibility (LHF). The interannual variability is driven more by

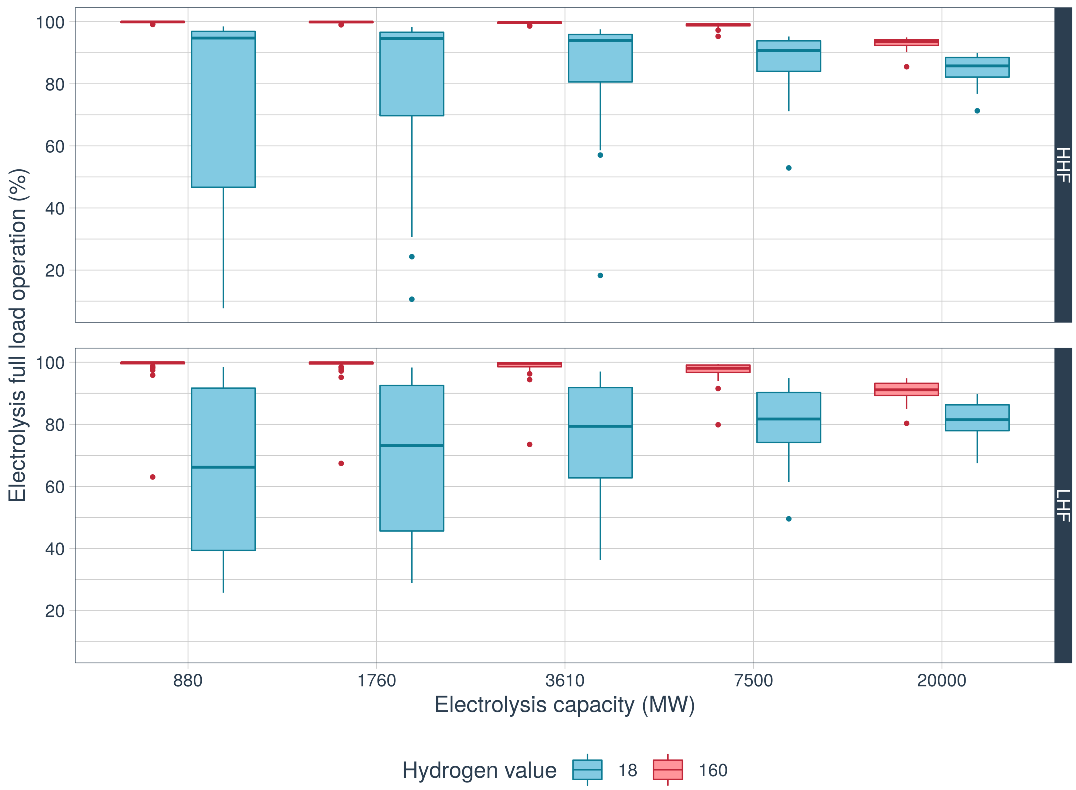


Figure 4: Electrolyzer full-load operation (%) for five different modelled hydrogen demand scenarios, and for both hydropower flexibility scenarios (top HHF, bottom LHF), over all 29 modelled weather years. The red boxes show the high hydrogen value scenario (thermal dispatch, 160 € $\mathrm{MWh}^{-1}$), and the blue the low hydrogen value scenario (no thermal dispatch, 18 € $\mathrm{MWh}^{-1}$).

hydropower than by wind power availability, as confirmed by the variability of the input data (figure 5).

It can also be seen that even for the high hydrogen value scenario, some of the 29 modelled weather years result in significantly reduced full-load hours, in particular in the LHF scenario. The outliers in the boxplot represent the weather years of 1987, 1996 and 2010, which were all cold years.

*3.2. Thermal power production and need for backup capacity*

Figure 6 shows load duration curves of the resulting dispatched thermal generation in two of the analysed hydrogen demand scenarios (NO and HIGH), for both analysed values of hydrogen, and for the two hydropower flexibility scenarios. The curves are derived from all 29 weather years (total of about 254,000 h). Naturally, a high value hydrogen results in significant dispatch of thermal generation (bottom panels), at increased levels compared to the NO hydrogen scenario (top). High hydrogen demand and low hydrogen value (middle panels), conversely, result in lower dispatched thermal generation, compared to the NO hydrogen scenario. Thermal dispatch here

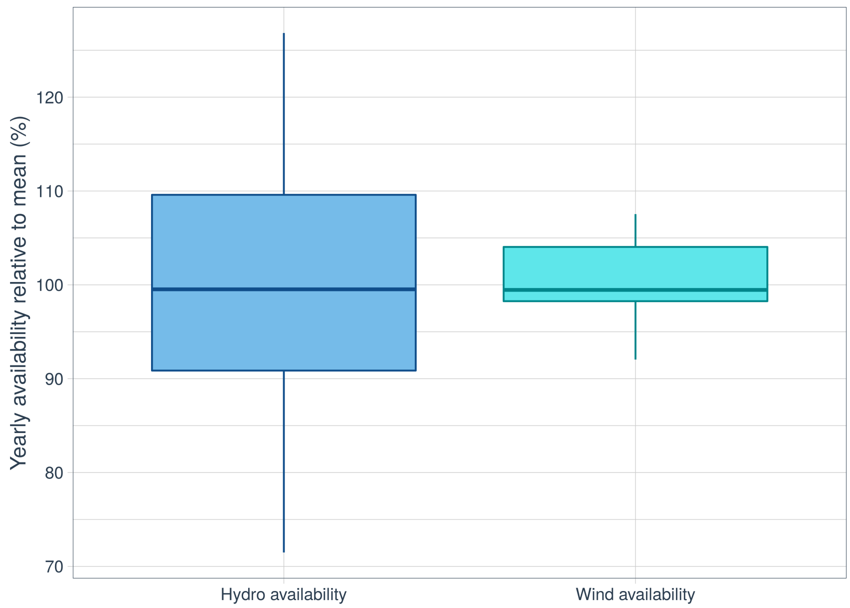


Figure 5: Variability of the input data for hydropower and wind power. Based on annual availability.

largely corresponds to the defined minimum production levels as determined by the heat demand from CHP plants, and fossil thermal (grey and yellow areas) is reduced to very few hours each year. Further, the thermal dispatch is, for obvious reasons, higher in the low hydropower flexibility scenario (right-hand panels), when in particular biomass-based CHP production has an important role to play in balancing the system.

Figure 7 shows the required backup capacity for the same six scenarios. The figure thus shows the parts of the residual demand not covered by thermal and hydropower generation, which means that additional backup measures are needed. The differences in the need for backup capacities between scenarios are similar to the patterns observed for thermal power production. In general, both the capacities and the full load hours are low. In the NO hydrogen scenario, about 6000 MW of backup capacity is required, which is reduced to just above 2000 MW in the HIGH hydrogen scenario. The capacities are dispatched for very few hours in the whole period - just over 1 % of all hours in the baseline scenario, which drops to less than 0.1 % in the HIGH hydrogen scenario.

### *3.3. Hydropower production and restrictions*

In figure 8 we show the resulting hydropower flows and ramping, for the hydrogen low value scenario, and for different hydrogen demands. When comparing this figure with figure 2, it is clear that both hydropower flexibility scenarios need to max out the allowed ramping at certain hours, but that the median ramping for both scenarios is well below the allowed levels. For the HHF scenario, the overall need for ramping decreases slightly with increasing hydrogen demand, whereas there is almost no difference in the LHF scenario. We also see larger flow variations in the HHF than in the LHF scenario, with not only lower minimum and median flows, but also a larger occurrence of higher flows.

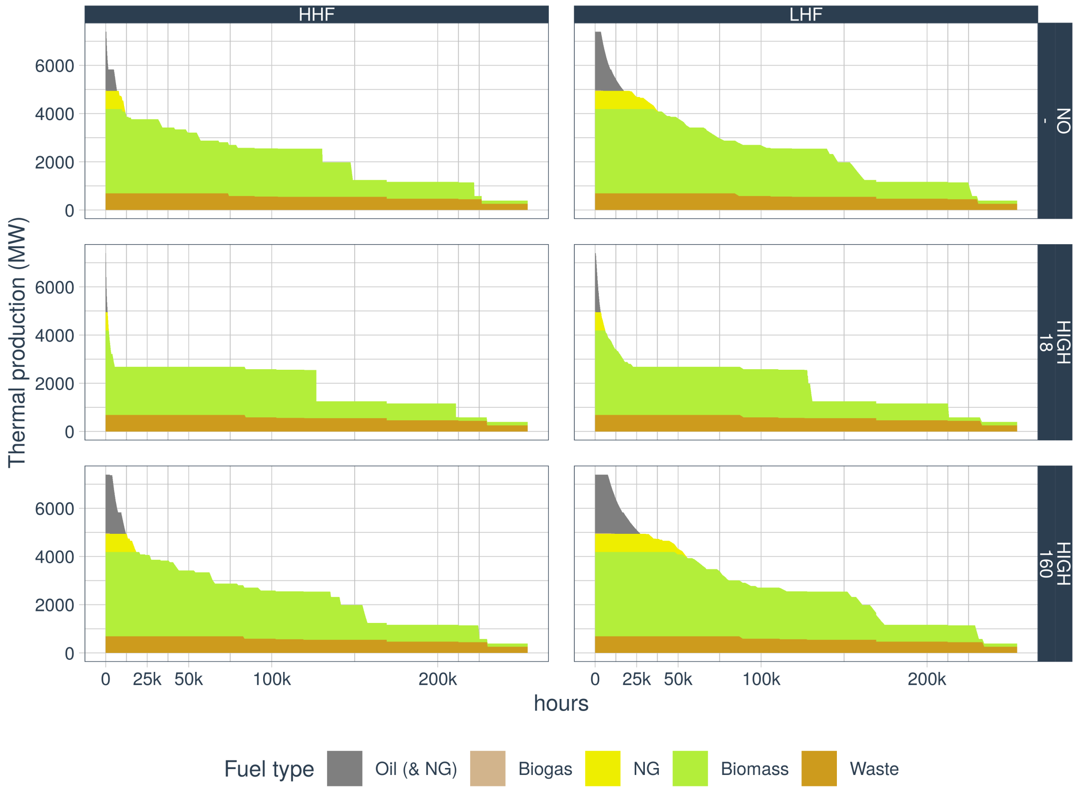


Figure 6: Resulting thermal power load duration curves, per production type (aggreggated), on hourly basis over all 29 years. Top: NO hydrogen scenario, middle: HIGH hydrogen at a value of 18 € MWh$^{-1}$, bottom: HIGH hydrogen at a value of 160 € MWh$^{-1}$. Left: HHF, right: LHF.

Another effect of restricting the hydropower flexibility is that more water will be spilled without passing through a turbine, which is shown in figure 9. The total hydro spilling increases significantly with the introduction of stricter environmental restrictions in the LHF scenario, compared to in the HHF scenario. This is apparent also in the HIGH hydrogen demand scenario, despite the significantly higher wind power capacity compared to in the NO scenario. Conversely, restricting the hydropower flexibility has little to no effect on the curtailment of wind power, as shown in the same figure.

From the results we can thus see that restriction of the hydropower, especially regarding allowed ramping (hydropeaking), has considerable effects on the power system, as both spilling, thermal dispatch and need for additional backup increases in the LHF compared to the HHF scenarios, irrespective of installed wind power capacity (i.e., hydrogen demand). As most of the allowed flexibility is not utilized fully, the trade-off in terms of environmental consequences of very few but potentially highly damaging extreme single events, must be weighed against the benefits for the power system.

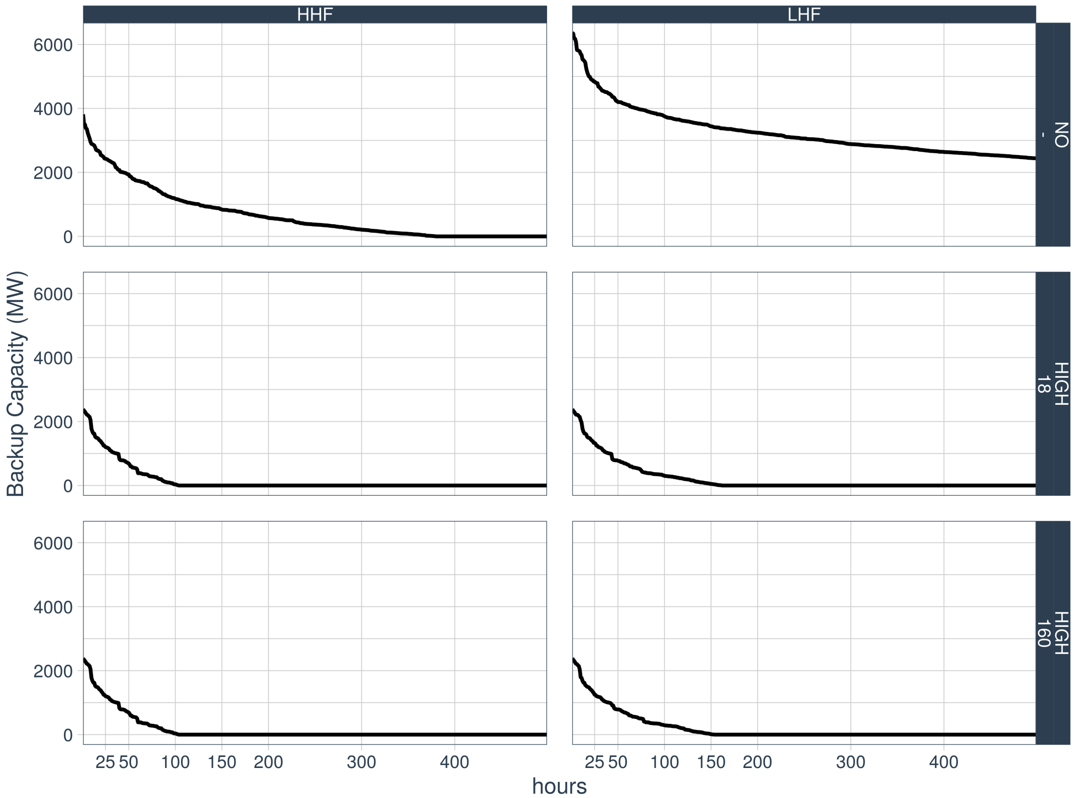


Figure 7: Load duration curves for additional backup capacity. Top: NO hydrogen, middle: HIGH hydrogen at a value of 18 € $\mathrm{MWh}^{-1}$, bottom: HIGH hydrogen at a value of 160 € $\mathrm{MWh}^{-1}$. Left: HHF scenario, right LHF scenario.

### *3.4. Trade-off analysis*

Within this section we show the explicit trade-offs in physical indicators between the scenarios (figure 10). The figure shows electrolyzer full load production, inter-annual variability of hydrogen production, thermal and backup volumes used (MWh $a^{-1}$), required backup capacity (MW), minimum hydro flow (MW), and mean hydro ramping (MW). All values are relatively scaled to the maximum of all scenarios, i.e., each bar shows the relative difference to the maximum value of that indicator among all analysed scenarios.

In the base scenario without hydrogen production (NO), a clear trade-off between restricting the hydropower flexibility on the one hand, and thermal volume and backup capacity and volume, on the other hand, can be observed. The strongest difference can be observed with respect to backup volume, which increases significantly in the LHF scenario. The backup capacity is also higher, but less significantly so.

This trade-off is maintained throughout the hydrogen demand scenarios. It can be observed that the backup capacities and volumes are always the same for the same hydropower flexibility scenario. Thermal dispatch for hydrogen production does thus not impact the required backup capacities, which hydropower flexibility does. For the HIGH hydrogen demand scenario, there is

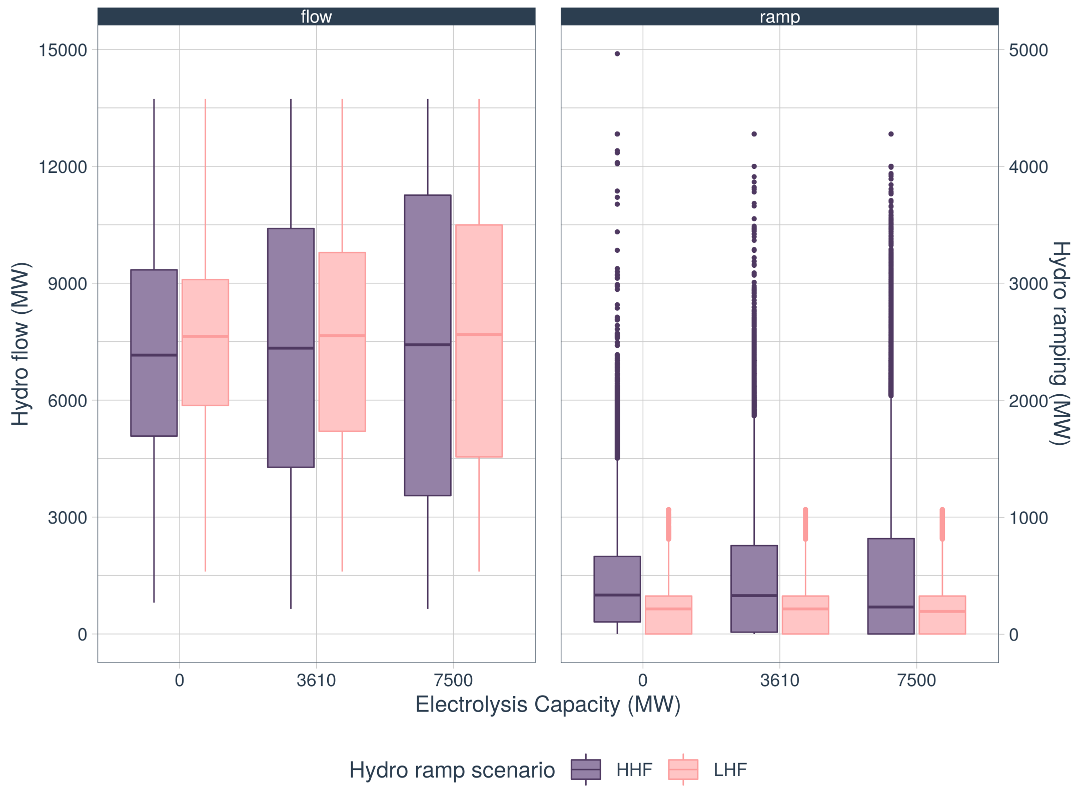


Figure 8: Resulting hydropower flow (left) and ramping (right) for the no thermal dispatch (18 € $\mathrm{MWh}^{-1}$) hydrogen value scenario and for different hydrogen demand scenarios.

actually no difference between any of the scenarios in terms of backup capacity, and only a marginal difference in the backup volume. These indicators become really low due to the high wind power penetration, which satisfies the demand in nearly all instances.

The resulting thermal volume differs between all scenarios: higher value of hydrogen and lower hydropower flexibility both increase the thermal volume. Observe that with increasing hydrogen demand, the thermal power production decreases compared to the NO scenario, for the low hydrogen value scenarios, as wind power substitutes thermal generation. Conversely, it increases for the high value scenarios, as thermal power is dispatched for electrolysis.

Of course, river flow indicators are always better (less ramping, higher minimum flow) in the LHF scenarios. Increasing the hydrogen demand has little impact on the ramping indicator, while the minimum flows decrease. This means that with increasing hydrogen demand, the minimum river flows can be expected to be reduced. The system is thus operated more flexibly, which causes a higher spread of the flows, even though both restrictions (minimum flow and maximum ramping) are satisfied. As hydropower is the only low cost flexibility option in the system, which is dispatched to produce hydrogen, it compensates for the increased variability of generation due to higher wind power shares.

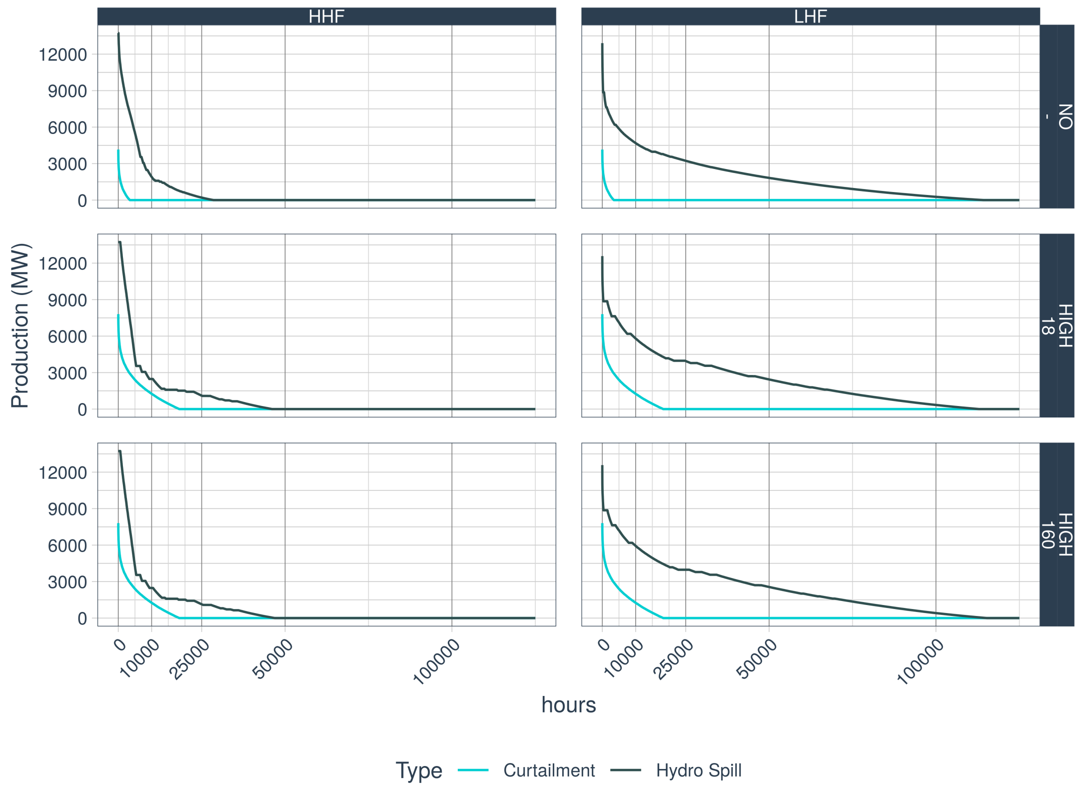


Figure 9: Duration curves curtailment of hydropower (HydroSpill) and wind (Curtailment) on hourly basis over all 29 years. Top: NO hydrogen, middle: HIGH hydrogen at a value of 18 € $MWh^{-1}$, bottom: HIGH hydrogen at a value of 160 € $MWh^{-1}$. Left: HHF scenario, right LHF scenario.

### *3.5. Sensitivity analysis*

Figure 11 shows the resulting full load hours when extending the modelled electrolyzer target capacity to very high levels (see section 2.2.1), which also means a related extension of the wind power capacity. The model was here also run with shorter capacity range step-size at lower capacities, in order to better capture the system behaviour at low capacities.

The figure shows that an increase of the electrolyzer capacity has a perhaps counter-intuitive behaviour: at the lower end of electrolyzer capacities, increasing capacities increases the full-load hours for the low hydrogen value scenarios, up to somewhere in the range of 5-10 GW of capacity, depending on the scenario. Above that point, adding more electrolyzer (and wind) capacity, reduces the full-load hours. The cause is that at lower wind capacities, wind is used to cover residual demand (as it is assumed to have zero marginal cost) in hours when there is a lot of wind. Less wind is thus available for surplus hydrogen production due to that substitution. Increasing the wind power capacity in the system further will reduce the thermal generation to the defined minimum load, thus making no more substitution of thermal generation possible and instead releasing a higher share


Figure 10: Trade off between indicators among all scenarios: the bars show the relative value of the indicator with respect to the maximum of that particular indicator among all scenarios.

of wind power generation for hydrogen production. Therefore, rapidly increasing full-load hours can be observed at the lower capacity range of the low hydrogen value scenarios. At some point, however, the negative load in the residual demand will exceed the electrolyzer capacity for some hours, which increases with the wind power capacity in the system. Once this effect grows stronger than the first effect, the full-load hours start decreasing again. This, however, applies only if no extra thermal power is dispatched for hydrogen production. In the high hydrogen value scenario, where thermal power is dispatched, the full-load hours start falling with increasing electrolyzer capacity immediately.

## 4. Discussion

We have here applied a dispatch model which does not take into account costs of investments into additional power generation or electrolyzers. Our model therefore cannot judge the economic feasibility of hydrogen production in such a system. In our low hydrogen value scenarios, we assumed that investment costs into generation capacities are not reflected in the market prices, as the market prices are determined by variable costs of thermal generation and by backup capacities only. In such a system, market prices would most of the time be very low or even close to zero, as zero variable cost technologies, i.e., wind and hydro power, would be price setting most of the

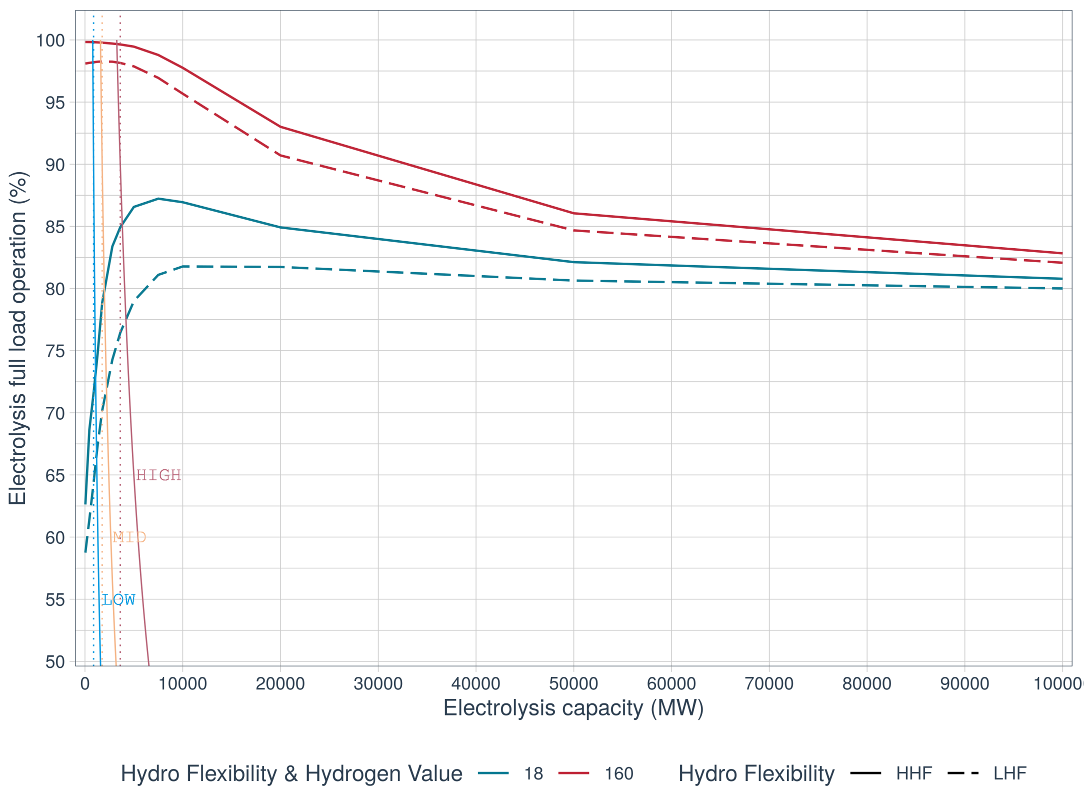


Figure 11: Average electrolyzer full-load operation (%) for an extended electrolyzer capacity range, for both hydropower flexibility scenarios: LHF and HHF, and for both hydrogen value scenarios: no thermal (18 € $MWh^{-1}$) and thermal dispatch (160 € $MWh^{-1}$). The three hydrogen demand scenarios are marked with vertical dotted lines, the curved lines shows the adjusted electrolyzer capacity to meet the expected yearly production (estimated at 90 % for each scenario).

time. This means that in particular wind power would have to recover investment costs from other sources of revenue, such as feed-in tariffs or market price premia.

We also assumed that Sweden has no international interconnections and that internally, there are no transmission bottlenecks. The first assumption makes our results conservative, as the existing interconnections clearly could provide backup capacities. At the same time, market prices and dispatch would change significantly, if interconnections would be taken into consideration. The reason is that, depending on the hydrogen value scenario, thermal power generation in neighbouring countries would be replaced up to the interconnector capacity, before generating surplus electricity for hydrogen production within the country. Disregard of international interconnections also means that Sweden is here a net zero exporter, which can be compared to the current annual exports of around 10-20 TWh of electricity.

The second assumption, which neglects internal restrictions in transmission, is of course a simplification. Here, our results depend on the final choice of placement of wind power capacity in Sweden. An implicit assumption is thus that jointly with the wind power expansion, the grid is enforced to prevent large-scale curtailments from wind power generation. We, however, assume that this occurs mostly in times of very high wind power generation, which is partly curtailed in our simulations too. In a well designed transmission system, the total effects should therefore be of minor scale.

Land and sea availability for placing wind-turbines is of course another major issue. In the scenario with the largest electrolyzer capacity (3610 MW), around 100 TWh of wind power is generated, causing an installation of around 30 GW of wind power capacity. This compares to an installed capacity of above 50 GW of wind in Germany, a country with only 80% of the available land area of Sweden. There should, thus, be no fundamental reason that restricts such an expansion. It will, however, cause regional environmental impacts and land conflicts, and mitigation measures must be taken seriously.

We here only considered increased load from the electrolysis - other scenarios show a potential increase from electrification of, e.g., transport and (other parts of) industry where total power demand may increase to over 200 TWh $a^{-1}$, including demand from electrolysis [11]. This compares to a load of about 130 TWh $a^{-1}$ in our scenario without electrolyzer and to around 160 TWh $a^{-1}$ in our largest electrolysis scenario. At the same moment, we assume that around 60 TWh $a^{-1}$ of nuclear are phased out. Keeping nuclear in the system, at least partly, would therefore be able to cover additional demands from other sectors.

Further, we modelled hydropower operation on an aggregated level for the whole of Sweden. Therefore, detailed assessments of environmental impacts are not possible. Also, some of the dispatch schedules may be physically impossible once down-scaled to the level of river basins. We recommend further work here.

## 5. Conclusions

We have here assessed the interactions in systems with combined thermal, hydro, and wind power, and large-scale introduction of electrolysis-based hydrogen production. The main trade-offs we have identified are between river flow indicators, and the required amounts of thermal generation and additional backup capacity. We emphasize, however, that being able to relieve the restrictions on hydropower flows in some moments when the system is particularly stressed, while maintaining stricter regulations for the residual time, may decrease this trade-off tremendously. Therefore, flexibility should be made flexible. Also, the trade-off between hydropower flexibility, and backup volumes and capacities, is low in absolute terms, for which reason the installation of additional backup measures comes at an overall low cost.

The second clear trade-off is between using thermal power generation and hydrogen production. The resulting electrolyzer full-load hours from our model are usually well above 60 or even 70%, depending on the scenario. However, in some years, the hydrogen production can decline drastically. To maintain stable flows to industrial users, dispatching thermal generation for hydrogen production in some years may therefore be necessary. Depending on the used fuel, this can cause significant $CO_2$-emissions in some years, but the overall impacts would be small.

There is also a sweet spot that minimizes the trade-off: when adding electrolyzers and the corresponding amounts of wind power generation to the system, while maintaining the thermal power generation at the same level or even decreasing it, electrolyzer full-load hours will first be low. They will, however, then increase up to the point where all potentially replaceable thermal power generation is actually replaced. After that point, electrolyzer full-load hours start declining again. The sweet spot is between 5 and 10 GW of electrolyzer capacity, where full-load hours of above 80% can be expected even without additional thermal generation.

In general, we conclude that a fully renewable electricity system in Sweden is possible at currently installed thermal and hydropower capacities, if (1) in total 50 TWh of wind power generation is available in the system, replacing 60 TWh of nuclear power generation and 10 TWh of exports, and (2) limited additional dispatchable backup capacities of around 6 GW are installed. The use of these backup capacities, in this scenario, is required in only a few hours in all simulated weather years. However, restricting hydropower flexibility makes a significant difference in terms of required thermal power generation and backup capacities.

**Acknowledgements**

The Swedish Research Council Formas (dnr. 2016-20118) and Bio4Energy financially supported this work. We also gratefully acknowledge support from the European Research Council ("reFUEL" ERC2017-STG 758149) and by CLIM2POWER. Project CLIM2POWER is part of ERA4CS, an ERA-NET initiated by JPI Climate, and funded by FORMAS (SE), BMBF (DE), BMWFW (AT), FCT (PT), EPA (IE), ANR (FR) with co-funding by the European Union (Grant 690462). We would also like to thank SMHI, the Swedish Meteorological and Hydrological Institute, for providing the S-Hype data.

**References**

[1] J. Michalski, M. Poltrum, U. Bünger, The role of renewable fuel supply in the transport sector in a future decarbonized energy system, International Journal of Hydrogen Energy 44 (25) (2019) 12554–12565. doi:10.1016/j.ijhydene.2018.10.110.
URL https://linkinghub.elsevier.com/retrieve/pii/S0360319918333093

[2] A. Otto, M. Robinius, T. Grube, S. Schiebahn, A. Praktiknjo, D. Stolten, Power-to-steel: Reducing CO2 through the integration of renewable energy and hydrogen into the German steel industry, Energies 10 (4). doi:10.3390/en10040451.

[3] E. S. Hanley, J. P. Deane, B. P. Gallachóir, The role of hydrogen in low carbon energy futures–A review of existing perspectives, Renewable and Sustainable Energy Reviews 82 (3) (2018) 3027–3045. doi:10.1016/j.rser.2017.10.034.

[4] I. Staffell, D. Scamman, A. Velazquez Abad, P. Balcombe, P. E. Dodds, P. Ekins, N. Shah, K. R. Ward, The role of hydrogen and fuel cells in the global energy system, Energy and Environmental Science 12 (2) (2019) 463–491. doi:10.1039/c8ee01157e.

[5] D. Ferrero, M. Gamba, A. Lanzini, M. Santarelli, Power-to-Gas Hydrogen: Techno-economic Assessment of Processes towards a Multi-purpose Energy Carrier, Energy Procedia 101 (September) (2016) 50–57. doi:10.1016/j.egypro.2016.11.007.
URL http://dx.doi.org/10.1016/j.egypro.2016.11.007https://linkinghub.elsevier.com/retrieve/pii/S1876610216312164

[6] C. J. Quarton, S. Samsatli, The value of hydrogen and carbon capture, storage and utilisation in decarbonising energy: Insights from integrated value chain optimisation, Applied Energy 257 (August 2019) (2020) 113936. doi:10.1016/j.apenergy.2019.113936.
URL https://doi.org/10.1016/j.apenergy.2019.113936https://linkinghub.elsevier.com/retrieve/pii/S030626191931623X

[7] T. Stocker, D. Qin, G.-K. Plattner, M. Tignor, S. K. Allen, J. Boschung, A. Nauels, Y. Xia, V. Bex, P. M. Midgley, Climate Change 2013: The Physical Science Basis, Cambridge University Press, Cambridge and New York, 2014.

[8] O. J. Guerra, J. Eichman, J. Kurtz, B.-M. Hodge, Cost Competitiveness of Electrolytic Hydrogen, Joule 3 (10) (2019) 2425–2443. doi:10.1016/j.joule.2019.07.006.

[9] G. Glenk, S. Reichelstein, Economics of converting renewable power to hydrogen, Nature Energy 4 (2019) 216–222. doi:10.1038/s41560-019-0326-1.
URL https://doi.org/10.1038/s41560-019-0326-1

[10] Swedish Government, Framework agreement between the Swedish Social Democratic Party, the Moderate Party, the Swedish Green Party, the Centre Party and the Christian Democrats (2016).
URL https://www.government.se/articles/2016/06/agreement-on-swedish-energy-policy/

[11] IVA, How the Swedish energy system manages the climate targets (Så klarar det svenska energisystemet klimatmålen, in Swedish), Tech. Rep. September, The Royal Swedish Academy of Engineering Sciences (IVA), Stockholm, Sweden (2019).
URL https://www.iva.se/globalassets/bilder/projekt/vagval-klimat/201910-iva-vagval-for-klimatet-delrapport5-g.pdf

[12] Swedish Energy Agency, 100 percent renewable electricity. Part report 2 (100 procent förnybar el. Delrapport 2 - Scenarier, vägval och utmaningar, in Swedish), Tech. rep., Swedish Energy Agency, Eskilstuna, Sweden (2019).

[13] Jernkontoret, Climate roadmap for a fossil-free and competitive steel industry in Sweden, Tech. rep., Jernkontoret, Stockholm, Sweden (2018).

[14] Swedenergy, The energy year 2018 - Electricity production (Energiåret 2018 - Elproduktion, in Swedish) (2019).

[15] IVA, Future Electricity Production in Sweden, IVA Electricity Crossroads project, Tech. rep., The Royal Swedish Academy of Engineering Sciences (IVA), Stockholm, Sweden (2017).
URL https://www.iva.se/globalassets/rapporter/vagval-el/201705-iva-vagvalel-framtidens-elproduktion-english-c.pdf

[16] I. Tobin, R. Vautard, I. Balog, F.-M. Bréon, S. Jerez, P. M. Ruti, F. Thais, M. Vrac, P. Yiou, Assessing climate change impacts on European wind energy from ENSEMBLES high-resolution climate projections, Climatic Change 128 (1-2) (2015) 99–112. doi:10.1007/s10584-014-1291-0.
URL http://link.springer.com/10.1007/s10584-014-1291-0

[17] I. Barstad, A. Sorteberg, M. dos Santos Mesquita, Present and future offshore wind power potential in northern Europe based on downscaled global climate runs with adjusted SST and sea ice cover, Renewable Energy 44 (2012) 398–405. doi:10.1016/j.renene.2012.02.008.
URL http://dx.doi.org/10.1016/j.renene.2012.02.008

[18] J. Olauson, M. N. Ayob, M. Bergkvist, N. Carpman, V. Castellucci, A. Goude, D. Lingfors, R. Waters, J. Widén, Net load variability in Nordic countries with a highly or fully renewable power system, Nature Energy 1 (12) (2016) 16175. doi:10.1038/nenergy.2016.175.
URL http://www.nature.com/articles/nenergy2016175

[19] S. Höltinger, C. Mikovits, J. Schmidt, J. Baumgartner, B. Arheimer, G. Lindström, E. Wetterlund, The impact of climatic extreme events on the feasibility of fully renewable power systems: A case study for Sweden, Energy 178 (2019) 695–713. doi:10.1016/j.energy.2019.04.128.
URL https://linkinghub.elsevier.com/retrieve/pii/S0360544219307613

[20] R. McKenna, Q. Bchini, J. Weinand, J. Michaelis, S. König, W. Köppel, W. Fichtner, The future role of Power-to-Gas in the energy transition: Regional and local techno-economic analyses in Baden-Württemberg, Applied Energy 212 (2018) 386–400. doi:10.1016/j.apenergy.2017.12.017.
URL https://linkinghub.elsevier.com/retrieve/pii/S0306261917317312

[21] B. Arheimer, G. Lindström, Electricity vs Ecosystems-understanding and predicting hydropower impact on Swedish river flow, IAHS-AISH Proceedings and Reports 364 (2014) 313–319. doi:10.5194/piahs-364-313-2014.

[22] F. B. Ashraf, A. T. Haghighi, J. Riml, K. Alfredsen, J. J. Koskela, B. Kløve, H. Marttila, Changes in short term river flow regulation and hydropeaking in Nordic rivers, Scientific Reports 8 (1) (2018) 1–12. doi:10.1038/s41598-018-35406-3.

[23] M. D. Bejarano, R. Jansson, C. Nilsson, The effects of hydropeaking on riverine plants: a review, Biological Reviews 93 (1) (2018) 658–673. doi:10.1111/brv.12362.
URL http://doi.wiley.com/10.1111/brv.12362

[24] B. M. Renöfält, R. Jansson, C. Nilsson, Effects of hydropower generation and opportunities for environmental flow management in Swedish riverine ecosystems, Freshwater Biology 55 (1) (2010) 49–67. doi:10.1111/j.1365-2427.2009.02241.x.
URL http://doi.wiley.com/10.1111/j.1365-2427.2009.02241.x

[25] M. D. Bejarano, Á. Sordo-Ward, C. Alonso, C. Nilsson, Characterizing effects of hydropower plants on sub-daily flow regimes, Journal of Hydrology 550 (2017) 186–200. doi:10.1016/j.jhydrol.2017.04.023.
URL https://linkinghub.elsevier.com/retrieve/pii/S0022169417302433

[26] M. Moreira, D. S. Hayes, I. Boavida, M. Schletterer, S. Schmutz, A. Pinheiro, Ecologically-based criteria for hydropeaking mitigation: A review, Science of the Total Environment 657 (2019) 1508–1522. doi:10.1016/j.scitotenv.2018.12.107.
URL https://doi.org/10.1016/j.scitotenv.2018.12.107

[27] N. L. R. Poff, J. C. Schmidt, How dams can go with the flow, Science 353 (6304) (2016) 1099–1100. doi:10.1126/science.aah4926.

[28] Swedish Energy Agency, Swedish Agency for Marine and Water Management, Stragey for measures in the hydropower (Strategi för åtgärder i vattenkraften - Avvägning mellan energimål och miljökvalitetsmålet Levande sjöar och vattendrag , in Swedish), Tech. rep., The Swedish Agency for Marine and Water Management, Göteborg, Sweden (2014).
URL www.havochvatten.se

[29] J. H. Halleraker, W. van de Bund, M. Bussettini, R. Gosling, S. Döbbelt-Grüne, J. Hensman, J. Kling, V. Koller-Kreimel, P. Pollard, Working Group ECOSTAT report on common understanding of using mitigation measures for reaching Good Ecological Potential for heavily modified water bodies. Part 1: Impacted by water storage, Tech. rep., European Union (2016). doi:10.2760/722208.

[30] S. Carr, G. C. Premier, A. J. Guwy, R. M. Dinsdale, J. Maddy, Hydrogen storage and demand to increase wind power onto electricity distribution networks, International Journal of Hydrogen Energy 39 (19) (2014) 10195–10207. doi:10.1016/j.ijhydene.2014.04.145.
URL http://dx.doi.org/10.1016/j.ijhydene.2014.04.145https://linkinghub.elsevier.com/retrieve/pii/S0360319914012038

[31] M. Korpås, C. J. Greiner, Opportunities for hydrogen production in connection with wind power in weak grids, Renewable Energy 33 (6) (2008) 1199–1208. doi:10.1016/j.renene.2007.06.010.

[32] E. Troncoso, M. Newborough, Electrolysers for mitigating wind curtailment and producing 'green' merchant hydrogen, International Journal of Hydrogen Energy 36 (1) (2011) 120–134. doi:10.1016/j.ijhydene.2010.10.047.
URL http://dx.doi.org/10.1016/j.ijhydene.2010.10.047

[33] R. Sarrias-Mena, L. M. Fernández-Ramírez, C. A. García-Vázquez, F. Jurado, Electrolyzer models for hydrogen production from wind energy systems, International Journal of Hydrogen Energy 40 (7) (2015) 2927–2938. doi:10.1016/j.ijhydene.2014.12.125.

[34] J. Olauson, M. Bergkvist, Modelling the Swedish wind power production using MERRA reanalysis data, Renewable Energy 76 (2015) 717–725. doi:10.1016/j.renene.2014.11.085.
URL http://dx.doi.org/10.1016/j.renene.2014.11.085https://linkinghub.elsevier.com/retrieve/pii/S0960148114008167

[35] J. Olauson, H. Bergström, M. Bergkvist, Scenarios and time series of future wind power production in Sweden, Tech. rep., Uppsala University, Uppsala (2015).

[36] G. Lindström, C. Pers, J. Rosberg, J. Strömqvist, B. Arheimer, Development and testing of the HYPE (Hydrological Predictions for the Environment) water quality model for different spatial scales, Hydrology Research 41 (3-4) (2010) 295–319. doi:10.2166/nh.2010.007.
URL http://hr.iwaponline.com/cgi/doi/10.2166/nh.2010.007https://iwaponline.com/hr/article/41/3-4/295/822/Development-and-testing-of-the-HYPE-Hydrological

[37] J. Strömqvist, B. Arheimer, J. Dahné, C. Donnelly, G. Lindström, Water and nutrient predictions in ungauged basins: set-up and evaluation of a model at the national scale, Hydrological Sciences Journal 57 (2) (2012) 229–247. doi:10.1080/02626667.2011.637497.
URL http://www.tandfonline.com/doi/abs/10.1080/02626667.2011.637497https://www.tandfonline.com/doi/full/10.1080/02626667.2011.637497

[38] Swedenergy, The energy year 2017 - Electricity production (Energiåret 2017 - Elproduktion, in Swedish), Tech. rep., Stockholm, Sweden (2018).

[39] Platts, UDI World Electric Power Plants Database (WEPP), Tech. rep. (2016).

[40] Bioenergi, Bio-power in Sweden (Biokraft i Sverige) 2018, Tech. rep. (2018).
URL `https://bioenergitidningen.se/e-tidning-kartor/biokraft-i-sverige`

[41] Swedenergy, Statistics over fuels and deliveries in Swedish district heating systems 2015-2017, Tech. rep., Stockholm, Sweden (2018).
URL `https://www.energiforetagen.se/statistik/fjarrvarmestatistik/tillford-energi/`

[42] I. Nohlgren, S. Herstad Svärd, M. Jansson, J. Rodin, El från nya och framtida anläggningar 2014, Tech. rep., Elforsk, Stockholm (2014).

[43] S. M. Saba, M. Müller, M. Robinius, D. Stolten, The investment costs of electrolysis – A comparison of cost studies from the past 30 years, International Journal of Hydrogen Energy 43 (3) (2018) 1209–1223. `doi:10.1016/j.ijhydene.2017.11.115`.

[44] O. Schmidt, A. Gambhir, I. Staffell, A. Hawkes, J. Nelson, S. Few, Future cost and performance of water electrolysis: An expert elicitation study, International Journal of Hydrogen Energy 42 (52) (2017) 30470–30492. `doi:10.1016/j.ijhydene.2017.10.045`.
URL `https://doi.org/10.1016/j.ijhydene.2017.10.045`

[45] L. Bertuccioli, A. Chan, D. Hart, F. Lehner, B. Madden, E. Standen, Development of Water Electrolysis in the European Union - Final report, Tech. rep., E4tech Sàrl and element energy, Lausanne, Switzerland and Cambridge, UK (2014).
URL `www.e4tech.com`

[46] Preem, Preem annual report 2018, Tech. rep. (2019).
URL `https://www.preem.se/globalassets/om-preem/finansiell-info/arsredovisningar/2018/preem{_}annual-report-2018{_}eng.pdf`

[47] J. A. Melero, J. Iglesias, A. Garcia, Biomass as renewable feedstock in standard refinery units. Feasibility, opportunities and challenges, Energy & Environmental Science 5 (6) (2012) 7393. `doi:10.1039/c2ee21231e`.
URL `http://xlink.rsc.org/?DOI=c2ee21231e`

[48] S. Karatzos, J. D. Mcmillan, J. N. Saddler, The Potential and Challenges of Drop-in Biofuels, Tech. rep. (2014).
URL `http://task39.sites.olt.ubc.ca/files/2014/01/Task-39-Drop-in-Biofuels-Report-FINAL-2-Oct-20`
`pdf`

[49] D. Kushnir, T. Hansen, V. Vogl, M. Åhman, Adopting hydrogen direct reduction for the Swedish steel industry: A technological innovation system (TIS) study, Journal of Cleaner Production 242. `doi:10.1016/j.jclepro.2019.118185`.

[50] M. A. Olivares, J. Haas, R. Palma-Behnke, C. Benavides, A framework to identify Pareto-efficient subdaily environmental flow constraints on hydropower reservoirs using

a grid-wide power dispatch model, Water Resources Research 51 (5) (2015) 3664–3680. doi:10.1002/2014WR016215.
URL https://onlinelibrary.wiley.com/doi/abs/10.1002/2015WR017200http://doi.wiley.com/10.1002/2014WR016215

[51] C. Mikovits, S. Höltinger, J. Schmidt, RE_EXTREME Simulation, Data, and Results (2020). doi:10.5281/zenodo.3712940.
URL https://zenodo.org/record/3712940

[52] IEA/NEA, Projected Costs of Generating Electricity, 2015 Edition, Tech. rep., International Energy Agency (IEA) and Nuclear Energy Agency (NEA), Paris, France (2015).
URL https://webstore.iea.org/projected-costs-of-generating-electricity-2015

[53] Sveriges Riksbank, Exchange rates, annual average 2018 (2019).
URL https://www.riksbank.se/en-gb/statistics/search-interest--exchange-rates/annual-average-exchange-rates/

[54] J. Gode, F. Martinsson, L. Hagberg, A. Öman, J. Höglund, D. Palm, Miljöfaktaboken 2011 - Estimated emission factors for fuels, electricity, heat and transport in Sweden (in Swedish), Tech. Rep. Report 1183, Stockholm (2011).

[55] Eurostat, Gas prices for non-household consumers (2018).
URL https://appsso.eurostat.ec.europa.eu/nui/show.do?dataset=nrg{_}pc{_}203{&}lang=en

[56] Swedish Energy Agency, Wood fuel- and peat prices, quarterly, 1993- (2019).

[57] European Commission, EU Weekly Oil Bulletin (2018).
URL https://ec.europa.eu/energy/en/data-analysis/weekly-oil-bulletin

## Appendix A. Model description

We employ a deterministic model to optimize the dispatch of hydropower and thermal power production. The model determines system costs minimizing the hourly dispatch costs of thermal power plants, while meeting the hourly demand. The program (*GAMS* & *Python*), the data necessary to run the simulations, the result files of the simulations discussed in this paper, and the *R* Code for result analysis can be found at Zenodo [51].

*Appendix A.1. Mathematical description*

*Appendix A.1.1. Objective*

The objective function is given by equation A.1, which represents dispatch costs $dispatch\_costs$ in the system over one year.

$$\begin{aligned} \min_{dispatch\_costs} \sum_h \Big( & x\_hydro_h \cdot c_{hy} + x\_spill_h \cdot c_s + \sum_{type} (x\_thermal_{h,type} \cdot c_{th,type}) \\ & + x\_backup\_dispatch_h \cdot c_{bd} - x\_h2_h \cdot p_{h2} \Big) \end{aligned} \tag{A.1}$$

The costs are given by the sum of dispatching thermal power production ($x\_thermal_{h,type}$) with cost $c_{th,type}$, and dispatching backup generation $x\_backup\_dispatch_h$ with cost $c_{bd}$. We also assign costs to hydropower production $x\_hydro_h$ and to spilling of water $x\_spill_h$. These costs are set very low and represent the future value of water. As the produced hydrogen $x\_h2_h$ has a market value $p_{h2}$, it enters negatively into the objective function.

*Appendix A.1.2. Constraints*

The residual demand $demand_h$, potential curtailments $x\_curtailment_h$, and hydrogen production has to be met in all time instances by generation of hydropower and thermal power as shown in equation A.2.

$$\begin{aligned} demand_h = x\_hydro_h + \sum_{type} (x\_thermal_{h,type}) + x\_backup\,demand_h \\ - x\_curtailment_h - x\_h2_h \qquad \forall h \end{aligned} \tag{A.2}$$

Installed capacities of thermal power plants $thcap_{type}$ and electrolyers $h2cap$ are defined in equations eqs. (A.3) and (A.4).

$$x\_thermal_{h,type} \leq thcap_{type} \qquad \forall h \tag{A.3}$$

$$x\_h2_h \leq h2cap \qquad \forall h \tag{A.4}$$

Additional constraints for hydro flow, ramping and the storage level are controlled with the following equations:
Equation A.5 ensures that the reservoir level $x\_reservoir\_level_h$ of one specific hour equals the

reservoir level of the previous hour, plus the natural inflow $natural\_inflow_h$, minus the outflow (hydro production $x\_hydro_h$ and spill $x\_spill_h$).

$$\begin{aligned} x\_reservoir\_level_h = {} & x\_reservoir\_level_{h-1} + natural\_inflow_h \\ & - x\_hydro_h - x\_spill_h \qquad \forall h \end{aligned} \tag{A.5}$$

The reservoir level $x\_reservoir\_level_h$ at the end of each simulated year is controlled by equation A.6, which ensures that the level is above $min\_endstorage$.

$$x\_reservoir\_level_h \geqslant min\_endstorage \quad h \in \{8760\} \tag{A.6}$$

The mimimum flow in each hour is controlled by equation A.7, which ensures that hydropower production $x\_hydro_h$ and hydro spilling $x\_spill_h$ is larger than the minimum flow $min\_flow_h$.

$$x\_hydro_h + x\_spill_h \geqslant min\_flow_h \qquad \forall h \tag{A.7}$$

Likewise, the maximum possible flow $max\_flow_h$ is defined by equation A.8.

$$x\_hydro_h + x\_spill_h \leqslant max\_flow_h \qquad \forall h \tag{A.8}$$

The maximum change in total flow per hour (maximum ramping, MRR) $max\_hydro\_ramp_h$ is defined by equations A.9 and A.10.

$$x\_hydro_h + x\_spill_h - x\_hydro_{h-1} - x\_spill_{h-1} \leqslant max\_hydro\_ramp_h \qquad \forall h \tag{A.9}$$

$$x\_hydro_{h-1} + x\_spill_{h-1} - x\_hydro_h - x\_spill_h \leqslant max\_hydro\_ramp_h \qquad \forall h \tag{A.10}$$

Maximum ramping $max\_hydro\_prod\_ramp$ of hydropower production $x\_hydro_h$ is controlled by equations A.11 and A.12.

$$x\_hydro_h - x\_hydro_{h-1} \leqslant max\_hydro\_prod\_ramp \qquad \forall h \tag{A.11}$$

$$x\_hydro_{h-1} - x\_hydro_h \leqslant max\_hydro\_prod\_ramp_h \qquad \forall h \tag{A.12}$$

Restrictions of thermal generation $x\_thermal_{h,type}$ are defined by the following equations. Minimum $min\_thermal_{h,type}$ and maximum $max\_thermal_{h,type}$ thermal generation by type are controlled by equations A.13 and A.14.

$$x\_thermal_{h,type} \geqslant min\_thermal_{h,type} \qquad \forall h, type \tag{A.13}$$

$$x\_thermal_{h,type} \leqslant max\_thermal_{h,type}, \qquad \forall h, type \tag{A.14}$$

Thermal ramping, summed over all types, is constrained by equations A.15 and A.16 .

$$\begin{aligned}\sum_{type}(x\_thermal_{h,type}) - \sum_{type}(x\_thermal_{h-1,type}) \\ \leqslant max\_thermal\_ramp_h \qquad \forall h\end{aligned} \tag{A.15}$$

$$\begin{aligned}\sum_{type}(x\_thermal_{h-1,type}) - \sum_{type}(x\_thermal_{h,type}) \\ \leqslant max\_thermal\_ramp_h \quad \forall h\end{aligned} \tag{A.16}$$

The hourly wind production $wind_h$ restricts wind curtailment $x\_curtailment_h$ in equation A.17, wind can thus be curtailed from 0 % to 100 %.

$$x\_curtailment_h \leqslant wind_h \qquad \forall h \tag{A.17}$$

*Appendix A.1.3. Parameters*

Table A.3 summarises the used hourly data, parameters and variables.

Table A.3: Hourly data, parameters and variables used.

| | Name | Symbol | Unit | Value |
|---|---|---|---|---|
| Hourly data | Residual demand | $demand_h$ | MW | see section 2.1.1 |
| | Natural in flow | $natural\_inflow_h$ | MW | see section 2.1.3 |
| | Wind production | $wind_h$ | MW | see section 2.1.2 |
| Costs & Values | Costs hydro generation | $c_{hy}$ | €MWh$^{-1}$ | 0.1 |
| | Costs hydro spilling | $c_s$ | €MWh$^{-1}$ | 0.05 |
| | Costs thermal generation by type | $c_{th,type}$ | €MWh$^{-1}$ | see table A.4 |
| | Costs backup generation | $c_{bd}$ | €MWh$^{-1}$ | 1500 |
| | Value hydrogen production | $p_{h2}$ | €MWh$^{-1}$ | 18‖160 |
| Capacities, Ramps & Restrictions | Thermal capacity by type | $thcap_{type}$ | MW | see table 1 |
| | Electrolysis capacity | $elcap$ | MW | see table 2 |
| | Minimum endstorage | $min\_endstorage$ | MW | 60 % of Reservoir capacity |
| | Reservoir capacity | - | MWh | 33,700,000 |
| | Minimum hydro flow | $min\_flow$ | MW | see figure 2 |
| | Maximum hydro flow | $min\_flow$ | MW | see figure 2 |
| | Maximum hydro production ramp | $max\_hydro\_prod\_ramp$ | MW | 4000 |
| | Minimum thermal production by type | $min\_thermal_{h,type}$ | MW | see figure 1 |
| | Maximum thermal production by type | $max\_thermal_{h,type}$ | MW | see figure 1 |
| | Maximum thermal ramping | $max\_thermal\_ramp_h$ | MW | 1500 |

*Appendix A.2. Input data for thermal power production costs*

Table A.4 summarizes the key plant data used to calculate the thermal power production costs, and table A.5 the fuel costs and fuel-related $CO_2$ emission factors.

Power production costs were set based on bottom-up technology and fuel specific projections of electricity generation costs [42, 52], and were adjusted to €$_{2018}$ using the average 2018 currency exchange rate of 1 € = 10.3 SEK [53] and updated fuel prices. The production costs include fuel costs including a $CO_2$-charge (50 €/ton$_{CO_2}$), costs for operation and maintenance (O&M), and heat credits, when applicable.

Table A.4: Technical data for the modelled thermal power plants [42, 52]. CHP = combined heat and power, RDF = refuse derived fuel, NG = natural gas, NGCC = natural gas combined cycle, FST = condensing steam turbine, OCGT = open cycle gas turbine, IC = internal combustion engine, S = small, M = medium, L = large, I = industrial. See table 1 for additional details.

| Production type | Power prod. (MW) | Heat prod. (MW) | El. efficiency (%) | Alfa value | Var. O&M (€ MWh$^{-1}$ fuel) | Fixed O&M (€ MWh$^{-1}$ el.) |
|---|---|---|---|---|---|---|
| Waste (CHP) | 20 | 78 | 20 | 0.256 | 5.26 | 215 |
| RDF (CHP) | 20 | 70 | 22 | 0.286 | 5.46 | 166 |
| Biomass I (CHP) | 80 | 180 | 33 | 0.444 | 2.63 | 37.0 |
| Biomass L (CHP) [a] | 80 | 180 | 33 | 0.444 | 2.63 | 37.0 |
| Biomass M (CHP) | 30 | 72 | 32 | 0.417 | 2.53 | 56.5 |
| Biomass S (CHP) | 10 | 28 | 28 | 0.357 | 2.44 | 89.7 |
| NGCC-L (CHP) | 150 | 115 | 53 | 1.30 | 0.78 | 19.5 |
| NGCC-M (CHP | 40 | 35 | 49 | 1.14 | 0.97 | 29.2 |
| NG-IC (CHP) | 1 | 1.2 | 41 | 0.833 | 3.9 | 0 |
| Oil/NG FST | 300 | 0 | 38 | - | 4.66 | 14.3 |
| Oil OCGT | 300 | 0 | 34 | - | 5.21 | 10.1 |
| Biogas IC (CHP) | 1 | 1.2 | 41 | 0.833 | 3.9 | 0 |

[a] This category also contains CHP plants currently using coal or peat as fuel (total installed capacity of 298 MW), as those were assumed to have been replaced by biomass CHP.

Table A.5: Energy carrier costs and $CO_2$ emission factors.

| Energy carrier | Price (€ $MWh^{-1}$) | $CO_2$ emissions (kg $CO_2$/MWh) [54] | Price source |
|---|---|---|---|
| NG (≤5 MWbr) | 39 | 205.2 | [55] |
| NG (≤150 MWbr) | 33 | 205.2 | [55] |
| NG (≥150 MWbr) | 27 | 205.2 | [55] |
| Biogas | 79 | 0 | [42] |
| Woody biomass | 20 | 0 | [56] |
| Waste | -12 | 133.2 | [42] |
| RDF | 2.5 | 86.4 | [42] |
| Oil | 36 | 266.4 | [57] |
| Heat, large plants | -24.4 | - | [42] |
| Heat, small plants | -39 | - | [42] |